Nanoscale Advances

Accepted Manuscript

This article can be cited before page numbers have been issued, to do this please use: G. Roy, A. R. Likhar and D. Asthana, *Nanoscale Adv.*, 2026, DOI: 10.1039/D5NA01038A.

ROYAL SOCIETY OF CHEMISTRY

rsc.li/nanoscale-advances

View Article Online
DOI: 10.1039/D5NA01038A

ARTICLE

Unravelling the Interplay between Structure, Self-Assembly Patterns, AIEE and Chiroptical Properties of NDI-bis-Cholesteryl Systems

Received 00th January 20xx,
Accepted 00th January 20xx

DOI: 10.1039/x0xx00000

Gargee Roy,[a] Aakash Ravikant Likhar [a] and Deepak Asthana[a]*

Naphthalene Diimides (NDI) offer exquisite optical and electronic properties and find a broad range of applications in various chemical and biomedical fields. However, due to their flat structure, at higher concentrations, the emission from NDIs gets severely quenched. The restoration of luminescence in such interesting class of molecules have been widely explored through the tuning of their optical properties via synthetic modification, supramolecular self-assembly and aggregation induced emission (AIE) techniques. Here, we aim at highlighting the role of spacer group in the tuning of the chiroptical properties of NDI through self-assembly approach, using a bis-cholesteryl diimide system. The three NDI-bis-cholesteryl systems have been prepared and their self-assembled structures, optical and chiral properties in monomeric and aggregated states have been studied. Microscopic investigations reveal almost identicle morphology in aggregates, however, quite different aggregational behaviour and chiroptical properties in ground and excited state are observed. Circular dichroism (CD) studies revealed an interesting medium controlled enhancement and reversal of chiral properties in the self-assembled structures.

Introduction

The distinctive use of non-covalent interactions leading to the formation of ordered and complex aggregates is the foundation for an imminent domain of chemistry referred to as supramolecular chemistry. Supramolecular self-assembly is an instinctive process that is usually triggered by the solvent polarity and is guided by relatively weak intermolecular forces namely hydrogen bonding, van der Waals forces, dipole–dipole interactions, and π - π stacking interactions. A small structural, or sometimes conformational differences induced by an external stimulus, may steer the intermolecular attractive forces in different directions and results in morphological and chirality transformations.[1-8] Self-assembled supramolecular structures from various functional molecular materials have been noted to possess improved and exceptional properties viable for device fabrication.[9-15]

Among various other organic scaffolds, naphthalene diimides (NDI) are perhaps the most extensively applied building blocks.[16, 17] Possibility of functionalization at both, bay and core positions, allows formation of various NDI-systems that find diverse applications in materials, and display interesting biological activities.[18-21] NDIs have been exploited predominantly in the field of organic electronics, sensing, light harvesting, opto-electronics, and other light-emitting devices.[22-32] NDIs can often be modified to produce well-organized nanoarchitectures thereby providing a control over desired photophysical properties.[16, 33-35] This property of NDI has been utilized to design various systems that exhibit aggregation induced enhancement of emission (AIEE), a much desired property that avoids concentration caused quenching.[36-40] Besides AIEE, another interesting property of fluorescent systems is circularly polarised luminescence (CPL), which requires chiral environment.[41] Naphthalene imide and naphthalene diimides have been proven to be noticeably useful in designing highly efficient organic CPL materials.[42-44]

It is well understood that NDIs tend to self-assemble via π - π stacking interactions, and the mode of supramolecular network formation, e.g. J- or H- type aggregates, plays a crucial role in the observed optical or chiroptical properties of NDI systems.[45-47] Therefore, gaining a deep understanding about the structural factors that may alter the optical properties in the bulk becomes ineluctable. In the past, various studies have been dedicated to find the correlation between molecular structure of NDI derivatives and resultant self-assembled nanostructures.[40, 48-52] Having information about possible molecular packing modes would help in attaining control over the long-range order in self-assembled nanostructures.

Forming diimides of naphthalenetetracarboxylic dianhydride (NTCDA) are not greatly explored for functional applications, instead, modification at the core positions has been used as major strategy to modulate optical and electronic properties of NDIs.[17, 53, 54] However, core substitution is a tedious and complicated process involving rigorous multistep synthesis. We focussed on functionalization of NTCDA through imide formation using cholesteryl units. Due to its benign nature, cholesteryl has been widely used as a hydrophobic unit in NDI

[a] Department of Chemistry, Ashoka University, Sonipat, Haryana, India, 131029.
Supplementary Information available: [details of any supplementary information available should be included here]. See DOI: 10.1039/x0xx00000x

and various systems where small structural variations have been utilized to tune the supramolecular and photophysical properties of the molecules.[48, 55-57] In polar environments and aqueous media cholesteryl unit incites the aggregation and facilitates a chiral bias to the molecular assembly owing to the availability of the multiple stereocentres.[58, 59]

Herein, we have prepared three NDI systems (**1**-**3**) having two cholesteryl units at imide positions connected through different type of spacer groups (Scheme-1). The spacer groups are chosen to provide tuneability in molecular packing. Molecules **1** and **2** have rigid linkers, whereas, molecule **3** has a four CH_2-groups long alkyl spacers that provides sufficient flexibility to the cholesteryl units. Molecules **3** having flexible linker, can have lots of adjustments during the molecular self-assembly to attain the most stable molecular packing scheme.

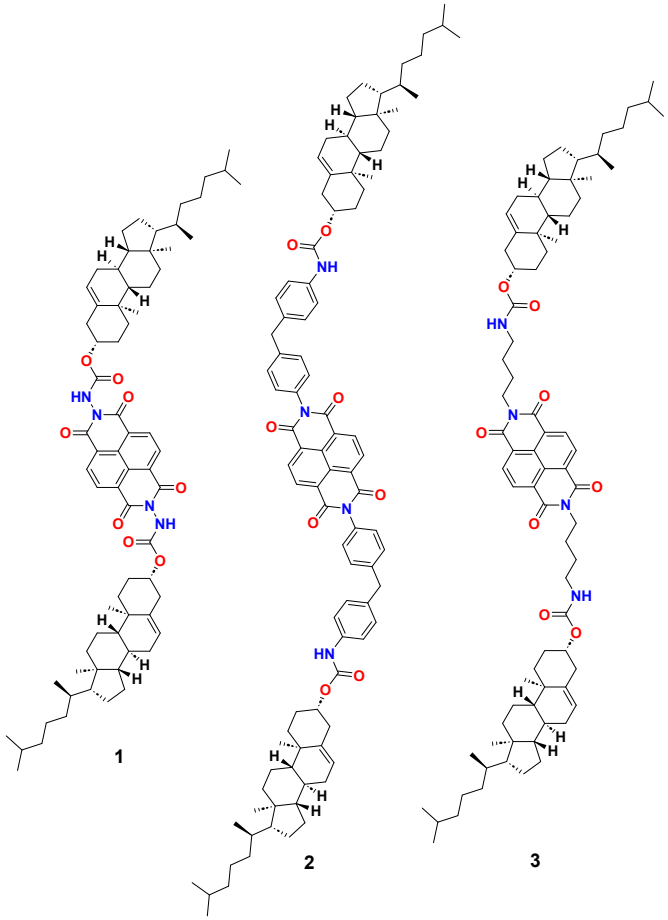

Scheme 1: Chemical structures of NDI derivatives (**1, 2** and **3**).

Results and discussion

Synthesis and characterizations

All the compounds were synthesized by following standard methods reported elsewhere. For preparation of compounds **1** and **2**, first cholesteryl chloroformate was reacted with hydrazine or 4, 4'-methylenedianiline to give mono-cholesterylcarboxylated intermediate products, which were then refluxed with NTCDA in dimethyl formamide (DMF) to give compounds **1** and **2**. In case of compound **3**, first an excess amount of 1,4-diaminobutane was reacted with Di-tert-butyl dicarbonate (Boc anhydride) to get tert-butyl (4-aminobutyl)carbamate, which was then refluxed with NTCDA in presence of DMF. Obtained diimide was treated with trifluoroacetic acid (TFA) to deprotect the amino group and then was reacted with cholesteryl chloroformate in dichloromethane in the presence of triethyl amine to produce compound **3**. All the compounds were then characterized by various analytical methods such as ^1H and ^{13}C NMR, mass spectrometry (MALDI) and FT-IR. The detailed synthetic procedure and characterization data can be found the supplementary information (SI) file.

Photophysical studies

Compounds **1**-**3** are designed to undergo self-assembly process in polar solvents. Molecular aggregation may lead to the formation of either *J* or *H*-type of assembly which can be investigated through optical measurements. In some cases, solvent may function as a trigger to switch the aggregate type. We carried out UV- Vis. absorption studies to explore the role of solvents in the aggregation behaviour of compounds **1**, **2** and **3**. As expected, all the three compounds show high solubility in less polar solvents like chloroform, dichloromethane etc. For our studies we chose tetrahydrofuran (THF) as solvent in which all compounds remain soluble at quite high concentration and it allows investigations to be performed in highly polar solvent mixture such as THF/H_2O. UV-Vis. absorption spectra of 20 µM solution of compounds **1**-**3** in THF showed characteristic absorption bands at around 340 nm, 355 nm and 375 corresponding to S_0-S_1 transitions and fine vibronic π–π^* transitions (Figure 1).[60, 61] Changing the solvent from polar THF to dichloromethane (DCM) affects the absorption spectra in an ununiform way (Figure 1d). In case of compounds **1** and **3**, we observed slight red shit and significant increase in absorbance, whereas, for compound **2**, there was a slight decrease in absorbance.

We noticed that addition of water in THF solution causes the solution to turn turbid due to the appearance of aggregated structures. We measured the absorption spectra of compounds **1**-**3** in THF/H_2O mixture and varied the water proportion to gain information about tuning of optical properties via self-assembly formation (ESI Figure S1). Initially, as the proportion of water is increased, the polarity increase in the solvent causes an increase in the absorbance with little shift in absorption bands (Figure 1 a-c). However, after reaching a certain percentage of water in the mixture, further increase results in a quick drop in absorbance, and this value (water percentage) differs for each compound. The observed slight red shift in absorption band could be attributed to the formation of *J*-type aggregates leading to offset π-stacking interactions. For compound **1**, when water reaches 45% in THF/H_2O mixture, a bathochromic shift of around 8 nm is noted. Similar trend is observed for compound **3**, however, the red shift is smaller (5 nm) and percentage of water required in THF/H_2O mixture to reach the transition point is much larger (60%). Surprisingly, in compound **2** the sudden

View Article Online
DOI: 10.1039/D5NA01038A

decrease in absorbance occurred at 35% water, showed no shift in absorption wavelength. At higher water percentages large aggregates started forming and sample lost its transparency.

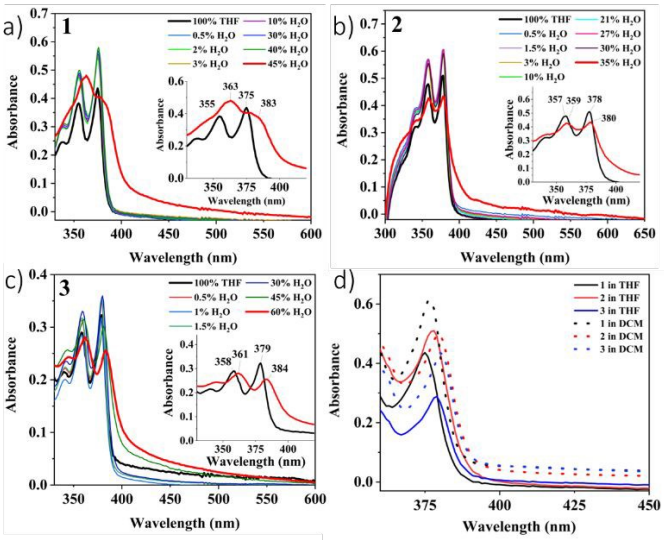

Figure 1: UV-Vis. absorption spectra of compounds **1**-**3** [20 µM] in THF/H_2O water solvent mixture (a-c), and in THF & DCM (d).

To have deeper insight in to polarity vs. aggregation induced changes, we further checked the absorption spectra of compound **3** in hexane and hexane/EtOH mixtures (Figure S1d). Increasing the EtOH in hexane/EtOH mixture resulted in continuous increase in absorbance with nearly no change in absorption band position. Changing ethanol from 40 to 60% in mixture showed decrease in absorbance, like one seen in THF/H_2O. Although, the absorbance follows similar trend in both THF/H_2O and Hexane/EtOH mixtures, no red shift in latter case negates the formation of *J*-type aggregates which are observed in the former.

To gain information about required water content in solvent mixture to trigger self-assembly, we performed concentration dependent UV-Vis. absorption study for molecule **1**. Absorption spectra of a 2 µM solution of **1** required 60% water to reflect the same bathochromic shift that is observed for a 20 µM solution in 45% water (Figure S1e). When a higher concentration sample is used [100 µM], the requirement of water proportion dropped to 40%.

We then started evaluating emission properties of these compounds. When excited at 370 nm, THF solutions of compounds **1**-**3** show fluorescence peaks centred around 421, 421 and 407 nm, respectively. Emission spectra of **1**-**3** in DCM revealed that the solvent polarity has significant influence on the fluorescence intensity of these compounds (Figure 2d). As can be seen, changing solvent from THF to DCM results in decrease in fluorescence intensity of compounds **1** and **2**. In contrast, compound **3** exhibited higher fluorescence intensity in DCM. As we have already seen from the absorption studies of compounds **1**-**3** the presence of water showed modulation of optical properties by triggering the self-assembly process. We performed the fluorescence measurements in THF/H_2O mixtures to understand the influence on aggregational behaviour on emission properties.

Fluorescence spectroscopy of compounds **1**-**3** [100 µM] in varying THF/H_2O solvent mixture revealed very interesting pattern in fluorescence intensities and confirmed the AIEE phenomenon in all three compounds (Figure 2a-c). When small amount of water is introduced in THF a quenching in fluorescence intensity is observed, which is expected for water.[62] For compound **1**, addition of merely 6% water causes a nearly 19% drop in fluorescence intensity (ESI Figure S3).This quenching is overcome by further addition of water. Due to the strong hydrophobic nature of the compound, increasing water proportion in the mixture initiates the self-assembly process. In aggregated form the AIEE becomes strongly favoured and fluorescence intensity starts to rise. Up to 30% water in THF/H_2O solvent mixture the fluorescence intensity remains lower than the fluorescence intensity observed in only THF, however, a drastic increase in intensity takes place when water was risen to 35%. At this level, fluorescence spectrum gets saturated.

Similar trend in fluorescence intensity change with respect to percentage of water in THF/H_2O are observed for compound **2** and **3** also (Figure 2b & c). For compound **2**, the initial fluorescence quenching due to added water is fully restored at around 20% water content. Further increase in water increases the fluorescence intensity. The sudden increase in intensity that is observed for **1** at 35%, occurs in the range of 25% to 27% for **2**. This implies stronger AIEE behaviour in compound **2**. The emission spectrum for compound **3** could not be measured under identical conditions, as the fluorescence intensity at 100 µM and slit width 20 mm (condition for measurement of compounds **1** & **2**) was too high to be measured. Therefore, for compound **3**, we kept the concentration same (100 µM) but decreased the slit width to 10 mm.

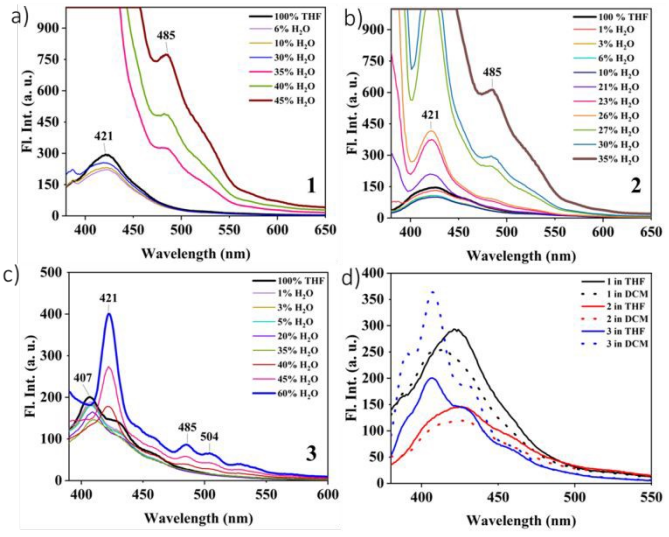

Figure 2: Emission spectra (λ_{exc}= 370 nm) of **1-3** [100 µM] in THF/H_2O solvent mixture (a-c), and in THF and DCM (d).

For compound **3**, the initial quenching due to addition of water was more severe than compounds **1** and **2** (Figure 2c), where

fluorescence intensity kept on decreasing until 35% water ratio. A slight red shift in emission wavelength was also noticed. It required 40% water in mixture to exhibit AIEE and finally 45% water was enough to make intensity higher than only THF case. An approximately 14 nm red shift in emission wavelength was also obvious to observe. The observed difference in their fluorescence behaviour and AIEE properties might be attributed to the difference in their structures that makes compound **3** more flexible allowing large adjustments in its supramolecular assembly than the compound **1** or **2**.

Having observed the strong aggregational behaviour of compound **1**-**3**, and considering the fact that cholesteryl unit usually favours supramolecular gel formation, we investigated the gelation ability of the synthesized compounds. To our surprize, all our attempts to find a gelation condition failed except one, in which we could get an opaque gel (2 wt%) of compound **3** in hexane/EtOH (1:6) mixture.

To have more information about AIEE properties, we measured the absolute Photoluminescence Quantum Yield (PLQY) of **1**-**3** in both dilute solutions and aggregated states. The PLQY values for **1, 2** and **3** in THF were found to be 6.2%, 4.4% and 14.0% respectively. PLQY values increases to 8.5%, 4.6% and 17.1% when measured in THF/H_2O mixture having 45% H_2O.

In general, NDI-based compounds bearing no substituents at core positions exhibit either no or very poor solid-state photoluminescence (SSPL) properties, except for a few systems.[44, 48, 49, 63, 64] As for any real life applications in form of devices it is desirable to have SSPL, we measured the emission spectra using powdered samples of **1**, **2** and **3** (Fig 3a). The spectra showed broad emission bands centred around at 417 nm, 421 nm and 454 nm, respectively. The observed SSPL peaks for compounds **1** and **2** are in close resemblance to the emission profile found in solution. However, for compound **3**, in the SSPL spectrum, a bathochromic shift of about 30 nm with respect to solution emission, is observed. Significant contribution from excimer emission might be the reason behind broadening of solid-state emission spectrum of **3**.

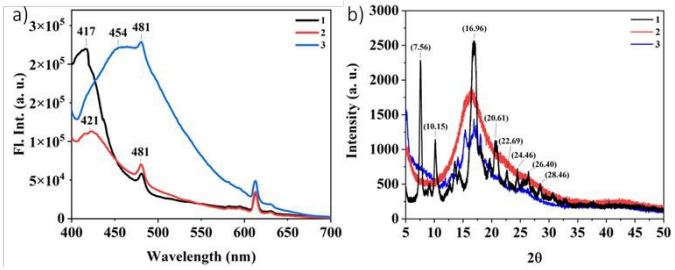

Figure 3: (a) SSPL spectra of powdered samples, and (b) PXRD spectra of compounds **1**-**3.**

We further examined the powder X-ray diffraction (PXRD) studies on compounds **1**-**3**. Among the three prepared bis-cholesteryl NDI derivatives, compound **1** showed more defined peaks indicating better crystallinity in the sample. Due to poor crystallinity, the peaks around 2θ= 25°-28°, which helps in predicting π- π stacking modes, are not well defined. Lack of those peaks in PXRD hint towards formation of *J*-type aggregates[65] which aligns with the UV-Vis. measurements.

In order to further delve into the understanding of AIEE, time-resolved photoluminescence (TRPL) measurements were done for all the three compounds in both the solution and aggregated states using different solvent combinations THF/H_2O and hexane/EtOH (Figure 4a-c). The excited-state fluorescence lifetime decay profiles (λ_{ex}= 370 nm) exhibited a bi-exponential decay pattern. Fluorescence lifetime in THF is found to be 1.25 ns, 1.82 ns and 1.54 ns for compounds **1**-**3**, respectively. Adding 20% water in THF resulted in an increase in lifetimes for all the three compounds. Increasing the water content further in the mixture, caused a decrease in lifetime. This shows faster decay in the aggregated state. We further checked the excited state lifetime for compound **3** in hexane/EtOH mixture, where it showed gelation properties, and observed the similar trend. Lifetime in hexane is found to be 1.23 ns which decreased to 1.13 ns and finally to 1.04 ns in 20% and 45% hexane/EtOH mixture, respectively.

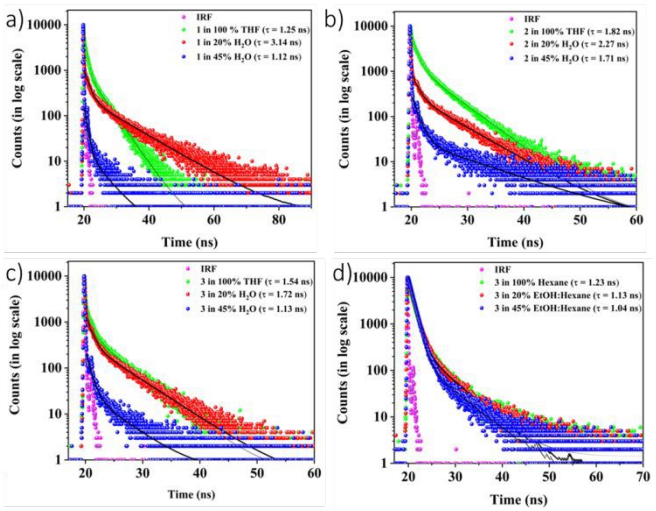

Figure 4: Plots showing fluorescence lifetime decay curves (λ_{ex}= 370 nm) and corresponding fit (solid black line) for compounds **1**-**3** [20 μM] in THF/H_2O (a-c), and for compound **3** in hexane/EtOH (d).

As compounds **1**-**3** are designed to have different linkages between naphthalene moiety and cholesteryl groups, we got interested in analysing the formed nanostructures to understand the impact of these structural differences on their self-assembled structures. Field Emission Scanning electron microscope (FE-SEM) images obtained from sample prepared from a [100 μM] solution of **1** and **2** in 10% H_2O/THF mixture revealed formation of cylindrical structures that are several micrometres in length (Figure 5). A closer look at those cylindrical rods like structure showed that they have a mesh like morphology. It is visible from the higher resolution images that self-assembled molecular aggregates further form intertwined network of nanostructures giving a rod-like appearances. In case of compound **3**, similar molecular aggregates are formed but they fail to attain any particular shape in the bulk.

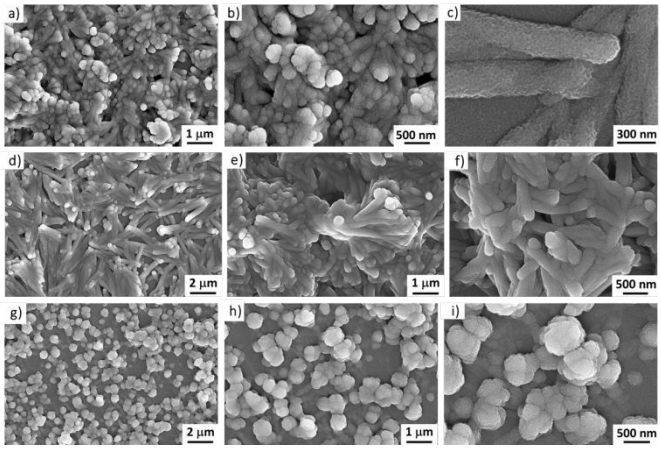

Figure 5: FE-SEM images obtained from a 10% THF/H_2O sample of **1** (a-c), **2** (d-f), and **3** (g-i).

Circular Dichroism (CD) and CPL Measurements

Inclusion of cholesteryl units in the molecular design introduces the chirality in the system. Chiral chromophores are of special interest for their chiroptical properties desirable for chiral sensing, switches, circularly polarized luminescence etc.[13, 66, 67] As Circular Dichroism (CD) spectrum provides an insight into the ground electronic state of a chiral compound, we measured the CD spectra of synthesized NDI-bis cholesteryl derivatives (**1**-**3**). To understand the effect of structure variation on overall chiral properties of these compounds, we performed measurements using aggregated samples obtained from [50 µM] solution in 50% THF/H_2O solvent mixture (Figure 6a). Under this condition, compound **1** showed a strong CD absorption band around 343 nm and 382 nm corresponding to the absorption bands of NDI moiety. The NDI absorption band for compounds **2** and **3** were there but weak in intensity. We further calculated the g_{abs} values for compounds **1**-**3**. For absorption peak at 250 nm, the g_{abs} shows a value of -0.028, +0.001, and -0.002, respectively. To clarify this, we measured the CD spectra of compounds **2** and **3** in higher concentration [100 µM] samples prepared in 50% THF/H_2O (Figure 6b). Interestingly, the sign of CD bands which is +ve for compound **2**, changes to -ve for compound **3**. This type of behaviour is usually observed in case of enantiomers where if one stereoisomer shows +ve then other stereoisomer shows -ve signal.

To correlate the observations made during investigation of self-assembly and its impact of emission spectra of compounds **1**-**3**, we performed CD measurements in THF and THF/H_2O mixture. For compound **1** [50 µM], we found that CD spectra remain very weak in both THF and 20% H_2O/THF solvent (ESI Figure S7a). However, when water proportion is doubled, making it 40% in H_2O/THF mixture, intensity of CD spectra increases dramatically between 325 nm to 425 nm, and gets saturated. CD spectra of compounds **2** and **3** [100 µM], in varying amount of water in THF/H_2O did show the increase in signal intensity, but the difference was not as remarkable as the one seen with compound **1** (ESI Figure S7a).

To understand the roles of polarity of the solvent medium on the overall chiral behaviour in the bulk, we further performed CD measurements in solvents with varying polarities. CD spectra of compounds **1**-**3** in DCM, 50% DCM/MeCN, 50% DCM/MeOH, DMF and 50% DMF/H_2O was recorded. In case of compound **1** [50 µM], the CD spectrum initially showed -ve CD signal centred around 350 nm, which became less -ve when solvent was changed to DMF, or 50% DCM/MeCN or DCM/MeOH. Upon changing the solvent to DMF, CD signal looked opposite to one observed in DCM, indicating a complete inversion of helicity (ESI Figure S7d). This is in agreement with the CD spectrum observed in 50% THF/H_2O where CD signal corresponding to NDI absorption band is +ve (Figure 6a).

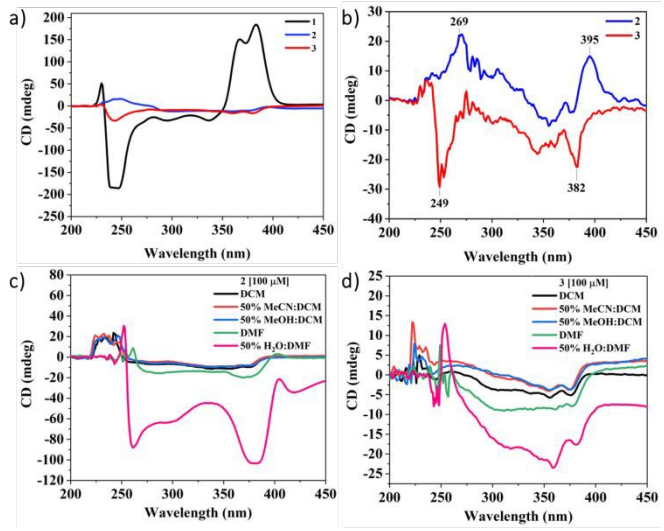

Figure 6: Room temperature CD spectra of in 50% THF/H_2O: (a) **1**-**3** [50 µM], (b) **2** and **3** [100 µM]. Plots (c) and (d) show CD spectra of compounds **2** and **3** [100 µM] in DCM, 50% DCM/MeCN, 50% DCM/MeOH, DMF, and 50% DMF/H_2O.

Similar CD measurements performed with compound **2** and **3** [100 µM] revealed very interesting results (Figure 6c-d). For compound **2**, while there was no significant change in CD signal intensity in changing solvent from DCM to 50% DCM/MeCN or DCM/MeOH, an increase in intensity was observed for DMF. However, drastic increase in signal intensity took place when solvent was changed to 50% DMF/H_2O (Figure 6c). CD signal signs are opposite to one observed in 50% THF/H_2O (Figure 6b). Therefore, reversal in helicity is observed for compound **2** as well. Compound **3** measured under similar conditions showed expected increase in signal intensity, but no reversal of CD signal sign was observed (Figure 6d). These results prove the role of solvent medium in deciding the helicity of self-assembled nano-structures in the bulk.

Seeing encouraging CD data and impressive AIEE behaviour, we got interested in exploring CPL activity of these compounds in solid and in various solution conditions. Using a JASCO CPL-300 CPL spectrometer, we performed measurements for compounds **1** and **3** in 1:1 THF/H_2O mixture, and compound **2** in a 1:1 DMF/H_2O mixture. Excitation at 350 nm failed to provide any detectable CPL signal for compounds **1**-**3**. We further investigated the solid-state CPL spectrum for compound **1** in the pellet form; however, this too could not exhibit any CPL activity. Therefore, although compounds **1**-**3** show interesting CD and AIEE properties, they lack the ability to emit circularly polarized

light. Further design modification would be required to achieve it.

Conclusions

To summarize, here we have prepared three symmetric NDI derivatives bearing two chiral units in the form of cholesteryl group at imide positions. The spacer, that connects cholesteryl group with nitrogen atom of the NDI, are varied. In compounds **1** and **2** the spacer provides a rigid linkage in which cholesteryl groups stay tightly fixed in a specified orientation. However, in compound **3**, in which four -CH_2 groups are used, the linkage remains very flexible and allows a lot of freedom to the cholesteryl groups. This structural difference affects the mode of packing in molecular self-assembly. Using water as trigger to initiate self-assembly process in THF/Water mixture, we have explored the impact of the small structural variation on the absorption, emission, and chiral properties of these systems. Interestingly, all these compounds show AIEE properties and we could also obtain the minimum amount of water in THF to trigger AIEE behaviour, e.g. for compound **1** [100 µM], changing water proportion from 30% to 35% results in sudden and a steep rise in fluorescence intensity. Additionally, although all three compounds carry the same chiral unit, cholesteryl groups, compound **1** exhibits strongest CD signals under identical measurement conditions. Another interesting feature that we observed that compounds **2** and **3** display opposite chirality in same solvent system. We also demonstrated that how THF/H_2O and DMF/H_2O can be used to change the helicity in the self-assembled nanostructures. This information may provide vital suggestions in designing new chiral fluorophore for AIEE and CPL systems.

Author contributions

GR synthesized the reported molecules and collected the data. GR and ARL analysed the data. DA supervised the project. All authors contributed to manuscript preparation.

Conflicts of interest

There are no conflicts to declare.

Data availability

The additional data including synthetic procedure and various analytical characterizations are provided in ESI. †

Acknowledgements

GR and ARL are thankful to Ashoka University for the doctoral research fellowship. We are thankful to CRF facility IIT Delhi & SATHI IIT Delhi, instrument facility at Shiv Nadar University, and USIC Delhi University for their support with material characterizations. We are thankful to Dr. Jatish Kumar and Arunima C., IISER Tirupati, for their help with the CPL measurements. The authors gratefully acknowledge the financial aid provided by Axis Bank to support this research work.

References

1. D. Asthana, J. Shukla, S. Dana, V. Rani, M. R. Ajayakumar, K. Rawat, K. Mandal, P. Yadav, S. Ghosh and P. Mukhopadhyay, *Chem. Commun.*, 2015, **51**, 15237-15240.
2. D. Ke, C. Zhan, A. D. Q. Li and J. Yao, *Angew. Chem. Int. Ed.*, 2011, **50**, 3715-3719.
3. W. Zhang and C. Gao, *J. Mater. Chem. A*, 2017, **5**, 16059-16104.
4. S.-Y. Qin, S.-S. Xu, R.-X. Zhuo and X.-Z. Zhang, *Langmuir*, 2012, **28**, 2083-2090.
5. J.-D. Ding, W.-J. Jin, Z. Pei and Y. Pei, *Chem. Commun.*, 2020, **56**, 10113-10126.
6. W. Liang, X. He, N. R. Reddy, Y. Bai, L. An and J. Fang, *Langmuir*, 2019, **35**, 9004-9010.
7. S. M. Wagalgave, D. DucLa, R. S. Bhosale, M. A. Kobaisi, L. A. Jones, S. V. Bhosale and S. V. Bhosale, *New J. Chem.*, 2018, **42**, 6785-6793.
8. Z. Wang, X. Xie, A. Hao and P. Xing, *Angewandte Chemie International Edition*, 2024, **63**, e202407182.
9. T. Aida, E. W. Meijer and S. I. Stupp, *Science*, 2012, **335**, 813-817.
10. M. Más-Montoya and R. A. J. Janssen, *Adv. Funct. Mater.*, 2017, **27**, 1605779.
11. H. Cheng, R. Liu, R. Zhang, L. Huang and Q. Yuan, *Nanoscale Adv.*, 2023, **5**, 2394-2412.
12. M. Liu, L. Zhang and T. Wang, *Chem. Rev.*, 2015, **115**, 7304-7397.
13. A. Sengupta, G. Roy, A. R. Likhar and D. Asthana, *Nanoscale*, 2023, **15**, 18999-19015.
14. S. De, D. Asthana, C. Thirmal, S. K. Keshri, R. K. Ghosh, G. Hundal, R. Kumar, S. Singh, R. Chatterjee and P. Mukhopadhyay, *Chemical Science*, 2023, **14**, 2547-2552.
15. X. Li, Q. Han, X. Li, R. Li, A. Wang, S. Liang, Y. Sang, J. Li, Y. Tian, Y. Yang, Q. Li, S. Bai and J. Li, *Nature Communications*, 2025, **16**, 6044.
16. S. V. Bhosale, M. Al Kobaisi, R. W. Jadhav, P. P. Morajkar, L. A. Jones and S. George, *Chem. Soc. Rev.*, 2021, **50**, 9845-9998.
17. N. Sakai, J. Mareda, E. Vauthey and S. Matile, *Chem. Commun.*, 2010, **46**, 4225-4237.
18. S. V. Bhosale, C. H. Jani and S. J. Langford, *Chem. Soc. Rev.*, 2008, **37**, 331-342.
19. V. Tumiatti, A. Milelli, A. Minarini, M. Micco, A. Gasperi Campani, L. Roncuzzi, D. Baiocchi, J. Marinello, G. Capranico, M. Zini, C. Stefanelli and C. Melchiorre, *J. Med. Chem.*, 2009, **52**, 7873-7877.
20. V. Pirota, S. Iachettini, C. Platella, P. Zizza, G. Fracchioni, S. Di Vito, A. Carachino, F. Battistini, M. Orozco, M. Freccero, A. Biroccio, D. Montesarchio and F. Doria, *Nucleic Acids Res.*, 2025, **53**.
21. A. A. Ahmed, R. Angell, S. Oxenford, J. Worthington, N. Williams, N. Barton, T. G. Fowler, D. E. O'Flynn, M. Sunose, M. McConville, T. Vo, W. D. Wilson, S. A. Karim, J. P. Morton and S. Neidle, *ACS Med. Chem. Lett.*, 2020, **11**, 1634-1644.

22. B. J. Jung, N. J. Tremblay, M.-L. Yeh and H. E. Katz, *Chem. Mater.*, 2011, **23**, 568-582.
23. F. Würthner and M. Stolte, *Chem. Commun.*, 2011, **47**, 5109-5115.
24. M. Sommer, *J. Mater. Chem. C*, 2014, **2**, 3088-3098.
25. F. Doria, A. Oppi, F. Manoli, S. Botti, N. Kandoth, V. Grande, I. Manet and M. Freccero, *Chem. Commun.*, 2015, **51**, 9105-9108.
26. V. K. Gawade, R. W. Jadhav, V. R. Chari, R. V. Hangarge and S. V. Bhosale, *Anal. Methods*, 2023, **15**, 3727-3734.
27. S. Wu, F. Zhong, J. Zhao, S. Guo, W. Yang and T. Fyles, *J. Phys. Chem. A*, 2015, **119**, 4787-4799.
28. F. S. Etheridge, R. Fernando, J. A. Golen, A. L. Rheingold and G. Sauve, *RSC Adv.*, 2015, **5**, 46534-46539.
29. H. F. Higginbotham, P. Pander, R. Rybakiewicz, M. K. Etherington, S. Maniam, M. Zagorska, A. Pron, A. P. Monkman and P. Data, *J. Mater. Chem. C*, 2018, **6**, 8219-8225.
30. L. J. Rozanski, E. Castaldelli, F. L. M. Sam, C. A. Mills, G. Jean-François Demets and S. R. P. Silva, *J. Mater. Chem. C*, 2013, **1**, 3347-3352.
31. K. Sugiyasu, N. Fujita and S. Shinkai, *Angewandte Chemie International Edition*, 2004, **43**, 1229-1233.
32. K. Murata, M. Aoki and S. Shinkai, *Chemistry Letters*, 2006, **21**, 739-742.
33. N. Ponnuswamy, G. D. Pantoş, M. M. J. Smulders and J. K. M. Sanders, *J. Am. Chem. Soc.*, 2012, **134**, 566-573.
34. A. Mukherjee and S. Ghosh, *Organic Mater.*, 2021, **3**, 405-416.
35. A. Das and S. Ghosh, *Chem. Commun.*, 2016, **52**, 6860-6872.
36. Y. Hong, J. W. Y. Lam and B. Z. Tang, *Chem. Commun.*, 2009, DOI: 10.1039/B904665H, 4332-4353.
37. X. Fang, H. Ke, L. Li and M.-J. Lin, *Dyes Pigm.*, 2017, **145**, 469-475.
38. P. Choudhury, S. Sarkar and P. K. Das, *Langmuir*, 2018, **34**, 14328-14341.
39. L. Zong, Y. Xie, C. Wang, J.-R. Li, Q. Li and Z. Li, *Chem. Commun.*, 2016, **52**, 11496-11499.
40. D. A. Shejul, S. M. Wagalgave, R. W. Jadhav, M. A. Kobaisi, D. D. La, L. A. Jones, R. S. Bhosale, S. V. Bhosale and S. V. Bhosale, *New J. Chem.*, 2020, **44**, 1615-1623.
41. J. Kumar, T. Nakashima and T. Kawai, *J. Phys. Chem. Lett.*, 2015, **6**, 3445-3452.
42. F. Salerno, J. A. Berrocal, A. T. Haedler, F. Zinna, E. W. Meijer and L. Di Bari, *J. Mater. Chem. C*, 2017, **5**, 3609-3615.
43. A. R. Likhar, A. Cheran, A. Sengupta, C. Dutta, J. Kumar and D. Asthana, *Chem. Commun.*, 2024, **60**, 9022-9025.
44. Y. Gao, L. Wang, X. Ma, R. Jin, C. Kang and L. Gao, *Chem. Eur. J.*, 2023, **29**, e202202476.
45. A. Eisfeld and J. S. Briggs, *Chem. Phys.*, 2006, **324**, 376-384.
46. A. P. Deshmukh, N. Geue, N. C. Bradbury, T. L. Atallah, C. Chuang, M. Pengshung, J. Cao, E. M. Sletten, D. Neuhauser and J. R. Caram, *Chem. Phys. Rev.*, 2022, **3**.
47. K. Cai, J. Xie, D. Zhang, W. Shi, Q. Yan and D. Zhao, *J. Am. Chem. Soc.*, 2018, **140**, 5764-5773.
48. C. Kulkarni and S. J. George, *Chem. Eur. J.*, 2014, **20**, 4537-4541.
49. A. Insuasty, S. Carrara, J. Xuechen, C. R. McNeill, C. Hogan and S. J. Langford, *Chem. Asian J.*, 2024, **19**, e202400152.
50. S. M. Wagalgave, S. D. Padghan, M. D. Burud, M. A. Kobaisi, D. D. La, R. S. Bhosale, S. V. Bhosale and S. V. Bhosale, *Sci Rep.*, 2019, **9**, 12825.
51. A. Sarkar, R. Sasmal, A. Das, A. Venugopal, S. S. Agasti and S. J. George, *Angew. Chem. Int. Ed.*, 2021, **60**, 18209-18216.
52. A. Das and S. Ghosh, *Macromolecules*, 2013, **46**, 3939-3949.
53. C. Röger and F. Würthner, *J. Org. Chem.*, 2007, **72**, 8070-8075.
54. S. V. Bhosale, S. V. Bhosale and S. K. Bhargava, *Org. Biomol. Chem.*, 2012, **10**, 6455-6468.
55. Z. Cao, F. Zhu, A. Hao and P. Xing, *J. Phys. Chem. C*, 2020, **124**, 7965-7972.
56. P. Xing, Y. Li, Y. Wang, P.-Z. Li, H. Chen, S. Z. F. Phua and Y. Zhao, *Angewandte Chemie International Edition*, 2018, **57**, 7774-7779.
57. J. Zhang, A. Hao and P. Xing, *Nano Letters*, 2024, **24**, 16191-16199.
58. H. Svobodová, V. Noponen, E. Kolehmainen and E. Sievänen, *RSC Adv.*, 2012, **2**, 4985-5007.
59. K. Yin, N. Feng, N. Godbert, P. Xing and H. Li, *J. Phys. Chem. Lett.*, 2023, **14**, 1088-1095.
60. H. Shao, J. Seifert, N. C. Romano, M. Gao, J. J. Helmus, C. P. Jaroniec, D. A. Modarelli and J. R. Parquette, *Angew. Chem. Int. Ed.*, 2010, **49**, 7688-7691.
61. M. A. Kobaisi, R. S. Bhosale, M. E. El-Khouly, D. D. La, S. D. Padghan, S. V. Bhosale, L. A. Jones, F. Antolasic, S. Fukuzumi and S. V. Bhosale, *Scientific Reports*, 2017, **7**, 16501.
62. G. E. Dobretsov, T. I. Syrejschikova and N. V. Smolina, *Biophysics*, 2014, **59**, 183-188.
63. M. Pandeeswar, H. Khare, S. Ramakumar and T. Govindaraju, *RSC Adv.*, 2014, **4**, 20154-20163.
64. S. Basak, N. Nandi, S. Paul and A. Banerjee, *ACS Omega*, 2018, **3**, 2174-2182.
65. A. Insuasty, S. Carrara, J. Xuechen, C. R. McNeill, C. Hogan and S. J. Langford, *Chemistry – An Asian Journal*, 2024, **19**, e202400152.
66. S.-W. Shao, P. Puneet, M.-C. Li, T. Ikai, E. Yashima and R.-M. Ho, *ACS Macro Lett.*, 2024, **13**, 734-740.
67. X. Zhang, J. Yin and J. Yoon, *Chem. Rev.*, 2014, **114**, 4918-4959.

View Article Online
DOI: 10.1039/D5NA01038A

Data Availability Statement: The data provided in main text and ESI supporting the findings of this research work are available from the corresponding author upon request.